(44) Keller, A.; Sawada, S. *Makromol. Chem.* **1964**, *74*, 190.
(45) Bassett, D. C.; Hodge, A. M. *Proc. R. Soc. London, Ser. A* **1981**, *A377*, 25.
(46) Stack, G.; Mandelkern, L.; Voigt-Martin, I. G. *Macromolecules* **1984**, *17*, 321.
(47) Holdsworth, P. J.; Keller, A. *J. Polym. Sci., Polym. Phys. Ed.* **1968**, *2*, 707.
(48) Frank, F. C. *Growth and Perfection of Crystals*; Doremus, R. H., Roberts, B. W., Turnbull, D., Eds.; Wiley: New York, 1958; p 529.
(49) Khoury, F.; Bolz, L. H. *Proc.—Annu. Meeting, Electron Microsc. Soc. Am.* **1980**, *38*, 242.

Conformation Aspect of Poly(γ-oleyl L-glutamate) with Long Flexible Side Chains As Studied by Variable-Temperature ^{13}C CP/MAS NMR Spectroscopy

Baijayantimala Mohanty,[†,§] Tadashi Komoto,[†,⊥] Junji Watanabe,[†]
Isao Ando,*,[†] and Toru Shiibashi[‡]

Department of Polymer Chemistry, Tokyo Institute of Technology, Ookayama, Meguro-ku, Tokyo, Japan 152, and Tokyo Research Laboratory, Japan Synthetic Rubber Co., Ltd., Higashi-Yurigaoka, Asao-ku, Kawasaki, Japan. *Received August 22, 1988; Revised Manuscript Received March 29, 1989*

ABSTRACT: ^{13}C CP/MAS NMR experiments are carried out for poly(γ-oleyl L-glutamate) with unsaturated long side chains, as a function of temperature, in order to elucidate conformational features in the liquid-crystalline state. The experimental results show that the main chain of the polymer takes a right-handed α-helical conformation within the temperature range from −40 to 80 °C, while the long side chains are in a mobile state above −40 °C.

Introduction

It has been demonstrated that for a series of α-helical poly(L-glutamate)s with n-alkyl side chains of various lengths (where n is the number of carbon atoms in the alkyl group = 4–18), n-alkyl side chains longer than n = 10 form a crystalline phase composed of paraffin-like crystallites together with the α-helical main-chain packing into a characteristic structure.[1] The polymers form thermotropic cholesteric liquid crystals by melting of the side-chain crystallites. In order to obtain detailed information about the structure and dynamics of these cholesteric liquid crystals, it is very essential to study the structures and motion of the main chains and side chains at various temperatures.

Most recently, high-resolution CP/MAS (cross polarization/magic angle spinning) NMR, which is powerful tool for the structural and dynamic analyses of polymers in the solid state,[2-5] has been successfully applied to the investigation of the main-chain and side-chain structures and molecular motion in poly(L-glutamate) with n-alkyl side chains (n = 18) at room temperature[6] and also at other temperatures[7] through the observation of ^{13}C NMR chemical shifts in the solid state. The data show that the main chain of poly(γ-n-alkyl L-glutamate) assumes a right-handed α-helical conformation irrespective of the variable side-chain length and the n-alkyl chains assume an all-trans zigzag conformation.[6,7] These studies show that variable-temperature (VT) ^{13}C CP/MAS NMR experiments have the potential to provide detailed insight into the molecular structure and dynamics of these polymers in the solid and liquid-crystalline states.

As a continuation of these investigations, the purpose of this work is to investigate the structure of poly(γ-oleyl L-glutamate) (POLLG) with unsaturated side chains (n = 18) in the liquid-crystalline state as a function of temperature. The transition temperature between the solid and liquid-crystalline states of poly(γ-n-octadecyl L-glutamate) (n = 18) (POLG) is about 60 °C. But in the present case, DSC measurement clearly indicates that the crystallization of the side chains in POLLG does not occur over the temperature range from −40 to 80 °C. Thus, the polymer is in the liquid-crystalline state over a wide range of temperatures compared with POLG, even though the side chains of both the polymers have the same number of carbons. We attempt to elucidate the conformational behavior of both the side chains and the main chains as a function of temperature through the use of VT ^{13}C CP/MAS NMR experiments.

Experimental Section

Materials. Poly(γ-oleyl L-glutamate) was synthesized by ester-exchange reactions between poly(γ-methyl L-glutamate) (M_v = 100 000) and oleyl alcohol as described in a previous paper.[1] The complete replacement of methyl groups by oleyl groups was confirmed by ^{1}H NMR.

Measurements. ^{13}C CP/MAS NMR spectra were measured by means of a Bruker MSL-400 NMR spectrometer (100.6 MHz) with a VT CP/MAS accessory at temperatures form −40 to 80 °C. The sample (ca. 200 mg) was contained in a cylindrical rotor made of ceramic materials and spun at 3 kHz. Contact time is 2 ms and repetition time 5 s. Spectral width and data points are 27 kHz and 8K, respectively. The ^{1}H field strength was 2.0 mT for both the CP and decoupling processes. The number of accumulations was 160–200. ^{13}C chemical shifts were calibrated indirectly with reference to the higher field adamantane peak (29.5 ppm relative to tetramethylsilane ((CH)$_4$Si)). The field was calibrated at each temperature point used in the NMR experiments. The experimental error for the chemical shifts is within about ±0.1 ppm for the sharp peaks but more than ±0.1 ppm for the broad peaks as described below.

The DSC measurements were performed with a Perkin-Elmer DSC calorimeter. Wide-angle X-ray patterns were recorded with a flat-plate camera by using a Rigaku-Denki X-ray generater.

Results and Discussion

Thermal Behavior of Poly(γ-oleyl L-glutamate). We first compare the thermal behavior of POLLG with that

---

[†] Tokyo Institute of Technology.
[‡] Japan Synthetic Rubber Co., Ltd.
[§] Permanent address: Baijayantimala Mohanty, AT/PO Kortal, Jagatsinghpur, Dist-Cuttack, Orissa, India.
[⊥] Present address: Department of Polymer Chemistry, Gunma University, Tenjin-cho, Kiryu-shi, Gunma, Japan 376.

0024-9297/89/2222-4451$01.50/0

Table I
^{13}C NMR Chemical Shifts of Poly(γ-oleyl L-glutamate) and Its Related Polymers in the Solid State at Various Temperatures

	^{13}C NMR chemical shift, ppm											
temp, °C	CO (amide)	CO (ester)	CH=CH	OCH$_2$	C$_\alpha$	C$_\gamma$	C$_\beta$	δ-CH$_2$	β-CH$_2$	int CH$_2$	α-CH$_2$	CH$_3$
				Poly(γ-oleyl L-glutamate)								
−40	176.0	*h*	*h*	64.9	56.7	31.0	*g*	*g*	*g*	31.0	*g*	15.0
−20	176.0	171.7	130.3	*h*	56.0	*g*	*g*	*g*	*g*	30.7	23.7	14.9
0	*h*	171.5	130.2	*h*	57.4	*g*	27.9	*g*	32.8	30.5	23.5	14.6
25	176.6	172.2	130.3	64.7	57.5	*g*	28.0	26.7	32.8	30.6	23.5	14.8
40	*h*	172.1	130.4	64.6	58.1	*g*	28.0	26.7	32.7	30.5	23.4	14.7
60	175.8	172.1	130.4	64.7	57.7	*g*	27.9	26.6	32.6	30.4	23.3	14.6
80	175.9	172.0	130.4	64.7	57.9	31.7	27.9	26.6	32.6	30.3	23.2	14.5
				Poly(γ-*n*-octadecyl L-glutamate)[c]								
27	176.0	172.1		64.7	57.7	31.5	28.0		34.7[a]	33.4[a]	25.2[a]	14.7
				Poly(γ-benzyl L-glutamate)[d]								
25	176	172		65	57	31			32.7[b]	30.6[b]	23.5[b]	(14.9)
				Polyethylene[e]								
25										33.2[a]		
										31.4[b]		
				Solid *n*-Alkane (*n*-C$_{22}$H$_{46}$)[f]								
25										34.4	26.1	15.0
				Liquid *n*-Alkane (*n*-C$_{20}$H$_{42}$)[f]								
25										31.9	22.6	14.1

[a] Crystalline component. [b] Noncrystalline component. [c] Reference 6; the main-chain conformation takes the right-handed α-helix form; ( ) is for film sample. [d] Reference 13; the main-chain conformation takes the right-handed α-helix form. [e] Reference 5. [f] Reference 7. [g] Not identified because of the overlap of peaks. [h] Not identified clearly.

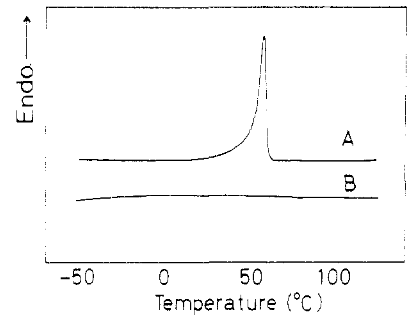

Figure 1. DSC heating curves of poly(γ-octadecyl L-glutamate) (A) and poly(γ-oleyl L-glutamate) (B).

of POLG reported previously.[1] As shown in the DSC thermogram (curve A) of Figure 1, POLG exhibited the first-order transition at around 60 °C, which was reproduced from the previous work.[1] The transition was attributed to the melting of the side-chain crystallites; the side chains having an all-trans zigzag conformation are long enough to crystallize independently on the rigid main-chain α-helices. Simultaneously with this transition, the α-helical rods take on the liquid-crystalline order because the long and flexible side chains can act like a solvent, undergoing rapid interconversions between the trans and gauche isomers. However, even though POLLG has a side chain of comparable length, no corresponding transition was observed in a temperature region above −40 °C, as shown in the DSC thermogram (curve B) of Figure 1. Hence, no crystallization of the side chains occurs in this case, as confirmed by the NMR results. Obviously, the double bond placed in the central part of the oleyl group interupts the crystallization of the side chains. Thus, the liquidlike nature of the side chains is demonstrated; the liquid-crystalline nature of α-helical rods may be maintained all the way to −40 °C. This is also identified by optical microscopy and X-ray diffraction measurements. A detailed study of the cholesteric liquid-crystalline properties of this material will be reported elsewhere.[7]

Conformational Aspects and ^{13}C NMR Behavior of Poly(γ-oleyl L-glutamate). Figure 2 shows the ^{13}C CP/MAS NMR spectrum of a POLLG sample at room temperature (25 °C). Assignment of peaks for the CO (amide), CO (ester), C$_\alpha$ and C$_\beta$ carbons is straightforward in view of reference data for poly(γ-benzyl L-glutamate) and poly(γ-*n*-alkyl L-glutamate) as examined previously,[6,7] and their chemical shift values are listed in Table I. We can identify a weak, broad CO (amide) peak, if we greatly expand and amplify the CO chemical shift region. The chemical shift values can be read from the top of the CO (amide) peaks. The experimental error may become as large as about ±0.5 ppm, this being a rough estimation. The low intensity of the CO (amide) peak may arise from the reduction of efficiency of the radiofrequency decoupling due to the reorientation of the main chain.[30] A similar phenomenon is observed in the VT ^{13}C CP/MAS NMR experiment of POLG.[7] The chemical shift value was read from this peak position as shown in Table I. As for the C$_\gamma$ carbon, the peak cannot be identified at low temperature because of overlap with the interior CH$_2$ carbon peak, but at high temperature (80 °C), it clearly appears due to the upfield shift of the interior CH$_2$ carbon peak. The assignment of the oleyl side-chain peaks is performed by reference to the data for POLG[6,7] and for *n*-alkanes and polyethylene as determined by VanderHart[8] and Ando et al.[5,9-12] and by solution-state ^{13}C chemical shift data,[8] as describe below. Upon careful examination, the interior CH$_2$ signal is found to split into two peaks of equal intensities above 25 °C, which overlap below 25 °C. The chemical shift difference between them is very small (0.3–0.4 ppm). From the stability of their intensity and chemical shift difference over a wide temperature range, from 25 to 80 °C, it is suggested that they arise from interior CH$_2$ carbons with two different chemical shifts. For example, there could be two different kinds of CH$_2$ carbons, one close to the double bond and the other relatively far away from it.

It has been demonstrated that ^{13}C chemical shifts of the CH$_2$ carbons in alkanes depend on the conformation and crystal structure;[5,8-13] similarly the carbon chemical shifts in polypeptides also depend on the main-chain conformation.[14-27] Therefore, much structural information about

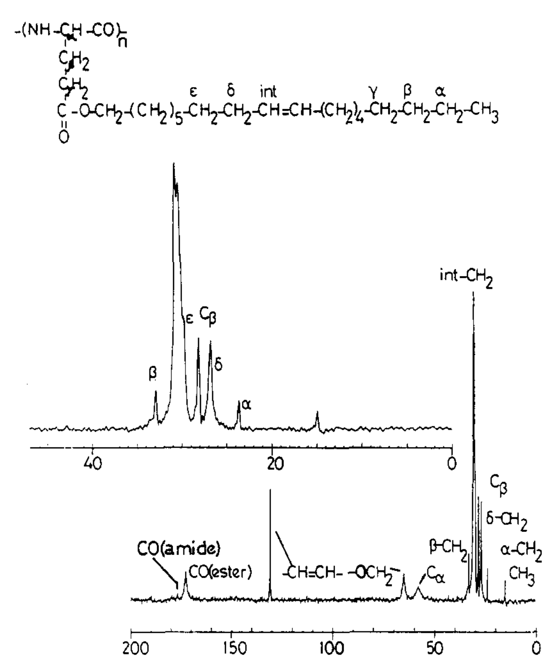

Figure 2. ^{13}C CP/MAS NMR spectrum of poly(γ-oleyl L-glutamate) in the solid state at room temperature. Peaks in the vicinity of 30 ppm are expanded. Assignment of each peak made from reference data of poly(γ-benzyl L-glutamate), poly(γ-*n*-octadecyl L-glutamate), and *n*-alkanes in the solid state (see the text).

the main chain and side chains of POLLG can be extracted from the observation of ^{13}C chemical shifts.

We have already demonstrated that the ^{13}C chemical shifts of the CO (amide) and C_α carbons for various polypeptides,[27] including poly(γ-benzyl L-glutamate), in the solid state are significantly displaced depending on the conformation, e.g., the right-handed and left-handed α-helix, ω-helix, and β-sheet forms. (For example, in the case of poly(γ-benzyl L-glutamate) the CO (amide) and C_α ^{13}C chemical shift values for the α-helix form are 176 and 57 ppm, respectively, and the corresponding values for the β-sheet form are 171 and 51 ppm, respectively.) Therefore, these ^{13}C chemical shift values can be effectively used for conformational studies of particular amino acid residues of polypeptides. In particular, CO (amide) chemical shifts are not strongly affected by residue structure and could be used to identify the main-chain conformation. The characteristic chemical shift values of right-handed α-helical poly(γ-benzyl L-glutamate) and POLG with similar side-chain structure to POLLG are listed in Table I, together with the chemical shift values of POLLG. As seen from Table I, ^{13}C chemical shift values for the CO (amide) and C_α carbons of poly(γ-benzyl L-glutamate) and POLG having a right-handed α-helix are about 176 and 57 ppm, respectively. On the other hand, the ^{13}C chemical shift values of CO (amide) and C_α carbons are 176.6 and 57.5 ppm, respectively, at room temperature. These values are very close to the characteristic values for the right-handed α-helix conformation in poly(γ-benzyl L-glutamate)[13] and POLG[6,7] in the solid state. Moreover, the ^{13}C chemical shifts of the C_β and CO (ester) carbons of POLLG are close to those of poly(γ-benzyl L-glutamate) and POLG. This means that the conformation of the inner part of the side chain in POLLG is the same as that of poly(γ-benzyl L-glutamate) and POLG.

We are also concerned with CH_2 peaks for the outer part of the side chain, which appear in the vicinity of about 30 ppm. The ^{13}C chemical shift data of *n*-alkanes, cyclic alkanes, and polyethylene can now be used to discuss the conformation and crystal structure of the side-chain CH_2 carbons.[8-12] It is reported that the CH_2 carbon signal in alkanes moves to high field by 4–6 ppm if any carbon atom three bonds away is in a gauche conformation rather than in a trans conformation.[28] This is known as the γ-effect. In fact, the CH_2 carbons of cyclic alkanes and *n*-alkanes in liquid or solution as well as those of polyethylene in the noncrystalline state appear at higher field by 2–3 ppm compared with those in the crystalline state[8-13] (see Table I). According to this empirical concept,[28] we can obtain information about the conformational behavior of the CH_2 carbons in the side chain through observation of the ^{13}C chemical shift. Let us look at the CH_2 signal regions carefully. In the spectrum at 25 °C, there is no significant peak corresponding to the crystalline state (34.4 ppm for n-$C_{22}H_{46}$ and 33.2 ppm for polyethylene); however, the interior CH_2 peak appears at 30.6 ppm. Based on the reference data on *n*-alkanes and polyethylene[8,27] (for example, 31.9 ppm for liquid n-$C_{22}H_{46}$ and 31.4 ppm for the noncrystalline component of polyethylene), this chemical shift value of the interior CH_2 carbons indicates that the CH_2 carbons are in a noncrystalline state.

Just as for the interior CH_2 carbons, the ^{13}C chemical shift value becomes a measure of the trans–gauche interconversions for the terminal α-CH_2 and β-CH_2 carbons in the side chain. The ^{13}C chemical shift values of the α-CH_2 and β-CH_2 carbons for n-$C_{22}H_{46}$ and POLG in the crystalline state (no molecular motion) are 25.2–26.1 and 33.4–34.4 ppm, respectively. On the other hand, when the trans–gauche conformational interconversion is rapid, the ^{13}C chemical shift values for these same carbons in liquid n-$C_{22}H_{46}$ and POLG in the noncrystalline state are 22.6–23.5 and 30.6–31.6 ppm. Therefore, there is a significant chemical shift difference between the terminal carbons of a side chain in the crystalline state and noncrystalline state. From these results it can be said that the α-CH_2 and β-CH_2 carbons in the side chains of POLLG in the liquid-crystalline state undergo fast trans–gauche interconversion at room temperature.

Figure 3 shows the ^{13}C NMR spectra of POLLG as a function of temperature; the ^{13}C chemical shift values are listed in Table I. The *n*-alkyl CH_2 peaks, whose nomenclature is defined in Figure 2, are found to change observably as the temperature is increased. There is no crystalline peak (in the vicinity of about 33 ppm) at −40 °C. As the temperature is increased from −40 to 80 °C, the intensity of the noncrystalline peak increases noticeably because of the decrease of linewidth due to an increase in the molecular motion. This shows that no crystallization of the side chains occurs within the measurement temperature range. The same results have been obtained from DSC and X-ray data.

The noncrystalline peak gradually shifts 0.7 ppm upfield from 31.0 to 30.3 ppm. Such behavior can be explained by the γ-effect concept[28]

$$\delta_{obs} = \delta_0 + 2\gamma f_g \tag{1}$$

where δ_{obs} and δ_0 are the observed ^{13}C chemical shift and the ^{13}C chemical shift for the trans conformation, respectively, f_g is the fractional gauche population, and γ is the chemical shift difference between the trans and gauche conformations (Tonelli[28] proposed $\gamma = -5.3$ ppm). In *n*-alkanes, the energy difference (E) between the trans and gauche conformations is about 600 cal/mol[31] and thus the increase of the fractional gauche population with increasing temperature from −40 to 80 °C can be estimated to be 0.09, where f_g can be approximated by using $f_g = 2\exp(-E/RT)/(1 + 2\exp(-E/RT))$ (R and T are the gas constant and the absolute temperature, respectively.). This increase

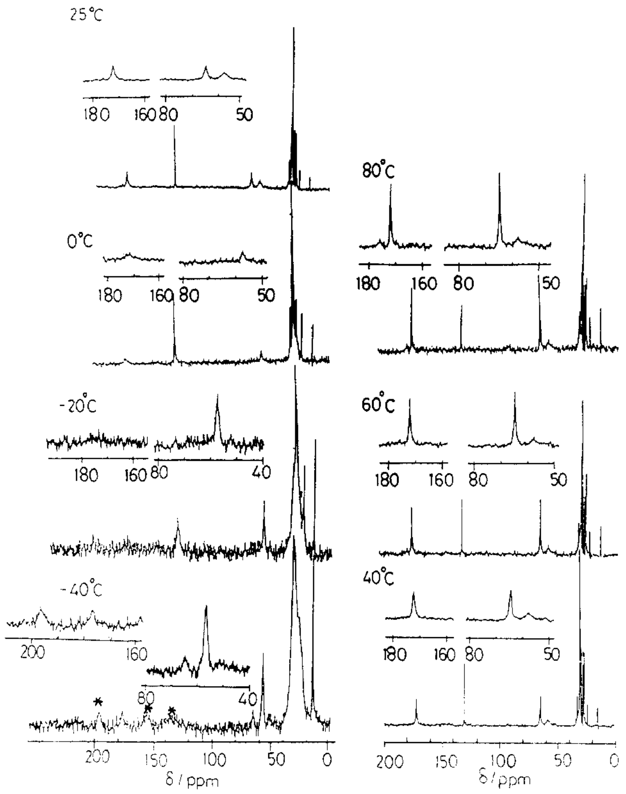

Figure 3. ^{13}C CP/MAS NMR spectra of poly(γ-oleyl L-glutamate) in the solid state as a function of temperature. The main-chain CO and C_α peak regions are expanded. * is for unknown peaks.

of the gauche population leads to an upfield shift of about 0.9 ppm. This is close to the observed value (0.7 ppm). This shows that the behavior of the trans–gauche transition of the side chains in POLLG is similar to that of *n*-alkanes.

For the CH_3, α-CH_2, and β-CH_2 carbons, also, as the temperature is increased, there are upfield shifts of 0.5 ppm (from −40 to 80 °C), 0.5 ppm (from −20 to 80 °C), and 0.2 ppm (from 25 to 80 °C), respectively. Chemical shift calculations, analogous to those for the interior CH_2 carbons, lead to predicted upfield shifts of 0.48, 0.44, and 0.2 ppm for the CH_3, α-CH_2, and β-CH_2 carbons, respectively. (The shift of the CH_3 carbon is larger than that for the β-CH_2 carbon because of the wider temperature variation of the former compared with the latter.) The calculated and observed results agree. This shows that the behavior of the trans–gauche interconversion of the CH_3, α-CH_2, and β-CH_2 carbons is similar to that of *n*-alkanes just as is the case for the interior CH_2 carbons. Further, we can identify a very slight upfield shift of about 0.1 ppm for the δ-cH_2 carbon upon increasing the temperature from 25 to 80 °C. This upfield shift can be explained in the same manner. However, the temperature-dependent shift for the δ-CH_2 carbon is very small. The contributions to the observed chemical shifts from changes in bulk density and bulk magnetic susceptibility, as well as changes in the average conformation, may become important. At this stage, however, we have neglected these contributions in the discussion. The ^{13}C chemical shift of CH=CH is almost independent of temperature. Such behavior differs from that of the interior CH_2 carbons, for which the temperature dependence of the chemical shift is large. Two possible reasons are considered. One is that there exists a considerably smaller γ-effect in the unsaturated carbon compared with that in the saturated carbon, and the other is that the conformational behavior in the vicinity of the CH=CH bond is different from that found in *n*-alkanes. At this stage it is not entirely clear which of these contributions is more important.

Finally, we are concerned with the temperature dependence of the ^{13}C chemical shifts of the main-chain carbons. The CO (amide) and C_α peaks are very broad and weak, probably because the correlation times for the backbone motions are in the appropriate range for producing significant line broadening.[30] We do not discuss this point further since we have not measured the relevant $T_{1\rho}$ parameters. We can read the ^{13}C chemical shift values from the broad and weak peaks with an experimental error (±0.5 ppm) that is larger than that for the other carbons (±0.1 ppm). The chemical shift values of the CO (amide) and C_α carbons are found to be 175.8–176.6 and 56.7–58.1 ppm at temperatures ranging from −40 to 80 °C, respectively. This shows that the main-chain carbon takes the right-handed α-helix conformation in the liquid-crystalline state over a wide range of temperatures.

From the above results, we conclude the following: First, the main-chain of POLLG assumes a right-handed α-helix within the temperature range from −40 to 80 °C, which is in the liquid-crystalline state. Second, there is no abrupt change in the conformation of the side chains over this temperature range. Further the side chains undergo fast interconversions between the trans and gauche isomers, and neither crystallize nor undergo any phase transition, even when the temperature is decreased to −40 °C.

Registry No. POLLG (homopolymer), 123438-51-7; POLLG (SRU), 123438-52-8.

References and Notes

(1) Watanabe, J.; Ono, H.; Uematsu, I.; Abe, A. *Macromolecules* **1985**, *18*, 2141.
(2) Schaefer, J.; Stejskal, E. O. In *Topics in Crbon-13 NMR Spectroscopy*; Levy, G. C.; Wiley: New York, 1979, Vol. 3, p 283.
(3) Fyfe, C. A.; Lyerla, J. R.; Volksen, W.; Yannoni, C. S. *Macromolecules* **1979**, *12*, 757.
(4) Lindberg, J. J.; Hortling, B. *Adv. Polym. Sci.* **1985**, *66*, 1.
(5) Ando, I.; Yamanobe, T.; Komoto, T.; Akiyama, S.; Sato, H.; Fujito, T.; Deguchi, K.; Imanari, M., *Solid State Commun.* **1987**, *62*, 785.
(6) Tsukahara, M.; Yamanobe, T.; Komoto, T.; Watanabe, J.; Ando, I.; Uematsu, I. *J. Mol. Struct.* **1987**, *159*, 345.
(7) Yamanobe, T.; Tsukahara, M.; Komoto, T.; Watanabe, J.; Ando, I.; Uematsu, I.; Deguchi, K.; Fujto, T.; Imanari, M. *Macromolecules* **1988**, *21*, 48.
(8) VanderHart, D. L. *J. Magn. Reson.* **1981**, *44*, 117.
(9) Ando, I.; Yamanobe, T.; Sorita, T.; Komoto, T.; Sato, H.; Duguchi, K.; Imanari, M. *Macromolecules* **1984**, *17*, 1955.
(10) Sorita, T.; Yamanobe, T.; Komoto, T.; Ando, I.; Sato, H.; Deguchi, K.; Imanari, M. *Makromol. Chem., Rapid Commun.* **1984**, *5*, 657.
(11) Yamanobe, T.; Sorita, T.; Ando, I.; Sato, H. *Makromol. Chem.* **1985**, *186*, 2071.
(12) Yamanobe, T.; Sorita, T.; Komoto, T.; Ando, I.; Sato, H. *J. Mol. Struct.* **1985**, *131*, 267.
(13) VanderHart, D. L.; Khoury, F. *Polymer* **1984**, *25*, 1589.
(14) Shoji, A.; Ozaki, T.; Saito, H.; Tabeta, R.; Ando, I. *Macromolecules* **1984**, *17*, 44.
(15) Taki, T.; Yamashita, S.; Satoh, M.; Shibata, A.; Yamashita, T.; Tabeta, R.; Saito, H. *Chem. Lett.* **1981**, 1903.
(16) Müller, D.; Kricheldorf, H. R. *Polym. Bull.* **1981**, *6*, 101.
(17) Saito, H.; Tabeta, R.; Shoji, A.; Ozaki, T.; Ando, I. *Macromolecules* **1983**, *16*, 1050.
(18) Saito, H.; Iwanaga, Y.; Tabeta, R.; Narita, M.; Asakura, T. *Chem. Lett.* **1983**, *427*.
(19) Saito, H.; Tabeta, R.; Asakura, T.; Iwanaga, Y.; Shoji, A.; Ozaki, T.; Ando, I. *Macromolecules* **1984**, *17*, 1405.
(20) Kricheldorf, H. R.; Müller, D. *Macromolecules* **1983**, *16*, 615.
(21) Ando, I.; Saito, H.; Tabeta, R.; Shoji, A.; Ozaki, T. *Macromolecules* **1984**, *17*, 457.
(22) Kricheldorf, H. R.; Mutter, M.; Müller, D.; Forster, H. *Biopolymers* **1983**, *22*, 1957.
(23) Saito, H.; Tabeta, R.; Ando, I.; Ozaki, T.; Shoji, A. *Chem. Lett.* **1983**, 1437.

Macromolecules **1989,** *22,* 4455–4462 **4455**

(24) Saito, H.; Kameyama, M.; Kodama, M.; Nagata, C. *J. Biochem.* **1982,** *92,* 233.
(25) Saito, H.; Tabeta, R.; Shoji, A.; Ozaki, T.; Ando, I.; Miyata, T. *Biopolymers* **1984,** *23,* 2279.
(26) Ando, S.; Yamanobe, T.; Ando, I.; Shoji, A.; Ozaki, T.; Tabeta, R.; Saito, H. *J. Am. Chem. Soc.* **1985,** *107,* 7648.
(27) Saito, H.; Ando, I. *Annu. Rep. NMR Spectrosc.* **1989,** *21,* 210.
(28) Tonelli, A. E.; Schilling, F. C. *Acc. Chem. Res.* **1981,** *14,* 223.
(29) Earl, W. L.; VanderHart, D. L. *Macromolecules* **1979,** *12,* 762.
(30) Lyerla, J. R.; Yannoni, C. S.; Fyfe, C. A. *Acc. Chem. Res.* **1982,** *15,* 208.
(31) Sheppard, N. J.; Szasz, G. J. *J. Chem. Phys.* **1962,** *17,* 86.

Real-Time Kinetic Study of Laser-Induced Polymerization

C. Decker* and K. Moussa

Laboratoire de Photochimie Générale (CNRS), Ecole Nationale Supérieure de Chimie de Mulhouse, 3 Rue Alfred Werner, 68200 Mulhouse, France. *Received February 2, 1989; Revised Manuscript Received April 14, 1989*

ABSTRACT: The photopolymerization of mono- and multiacrylic monomers, induced by continuous laser irradiation at 363.8 nm, has been studied by using the newly developed real-time infrared (RTIR) spectroscopy. The polymerization profiles were directly recorded in the millisecond time scale, thus allowing a precise evaluation of the reaction rate, the photosensitivity, the polymerization quantum yield, the induction period, and the polymer unsaturation content. The effect of the photoinitiator, the monomer functionality, and atmospheric oxygen is substantial and was quantified. The system that performed best contains 2,2-dimethoxy-2-phenylacetophenone as photoinitiator, a polyurethane diacrylate oligomer, and a [(dimethylmethoxy)formamido]ethyl monoacrylate monomer. Polymerization was shown to develop mainly in the dark, after the short laser exposure, especially in the early stages of the reaction, where the postpolymerization effect was found to represent up to 90% of the total process. For the more reactive photoresist, the overall polymerization quantum yield was measured to be 3000 mol photon^{-1} in the presence of air and 13 000 mol photon^{-1} for N_2-saturated systems, corresponding to a photosensitivity of 0.7 and 0.17 mJ cm^{-2}, respectively.

Introduction

Much effort has been devoted to photopolymers over the past few years because of the distinct advantages of UV radiation initiation, mainly, the rapidity of the reaction, which lasts a fraction of a second, and the selectivity, which permits high-resolution imaging. In the continuing search for ever faster polymerizing systems, lasers have appeared recently as one of the most powerful tools to transform rapidly a liquid monomer into a solid polymer.[1–9] Pulsed lasers, which deliver a large amount of energy within a few nanoseconds, have been often employed in polymer science, in particular to obtain kinetic rate constants for free-radical polymerizations[10–14] and to evaluate the effects of the pulse frequency on the molecular weight distribution.[15–18] Continuous output lasers still present the unique advantage of providing extremely high rates of initiation that remain essentially constant throughout the polymerization. Owing to the spatial coherence of the laser beam, complex polymer patterns can be directly written onto photosensitive plates at micronic resolution.[5]

One of the critical unsolved problems in laser-initiated polymerization is finding an adequate method to study in real time the kinetics of polymerizations which develop in the millisecond range. None of the usual analytical techniques has been able to meet this challenge so far. Conventional infrared spectroscopy has proved to be valuable for evaluating the polymerization extent after a short laser exposure,[4,5] but it is based on discrete measurements and includes in the final result the postpolymerization which develops just after the UV exposure. Differential scanning calorimetry is commonly used to monitor in real time the kinetics of light-induced polymerization,[6–8] but it was found inadequate in the present case due to its response time of a few seconds. The same holds true for other techniques such as dilatometry,[19,20] IR radiometry,[21] photoacoustic spectroscopy,[22] and nephelometry.[23,24] Laser interferometry,[25] a novel method based on refractive index changes upon polymerization, was shown to be well-suited for recording polymerization profiles in the millisecond time scale, but it provides no quantitative data about the rate of the reaction and the actual degree of polymerization.

Recently, a new analytical method, based on IR spectroscopy, has been developed in our laboratory in order to follow quantitatively and in real time photopolymerizations that take place in a fraction of a second.[26] In this paper, we describe how this technique was used to study the kinetics of polymerizations initiated by continuous-wave laser beams and thus evaluate polymerization rates and quantum efficiencies for various photoresists commonly used in UV-curable coatings and adhesives. It also reports the remarkable performance of a novel acrylic monomer that contains a carbamate function in its formula and has the unique advantage of polymerizing both rapidly and extensively.

Experimental Section

Materials. The photopolymerizable resins used in this work contained three main components: (i) a photoinitiator that cleaves readily upon laser exposure to generate free radicals (for most experiments, 2,2-dimethoxy-2-phenylacetophenone (Irgacure 651 from Ciba Geigy) was selected because of its high initiation efficiency; (ii) an acrylate end-capped oligomer consisting of an aliphatic polyurethane (Actilane 20 from SNPE) or of a derivative from the glycidyl ether of bisphenol A (Actilane 72 from SNPE); (iii) a reactive acrylic diluent, such as hexanediol diacrylate (HDDA from UCB), trimethylolpropane triacrylate (TMPTA from UCB), ethyl diethylene glycol acrylate (EDGA from SNPE), or [(dimethylmethoxy)formamido]ethyl monoacrylate (Acticryl CL 960 from SNPE), with the following formula:

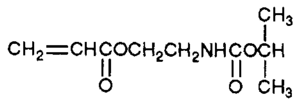

$$\mathrm{CH_2{=}CH\underset{\overset{\|}{O}}{C}OCH_2CH_2NH\underset{\overset{\|}{O}}{C}O\overset{CH_3}{\underset{CH_3}{CH}}}$$

Typical photoresist formulations contained 5% of initiator (0.2 mol L^{-1}) and equal parts of the acrylic oligomer and diluent. Some experiments were carried out with the diluent plus photoinitiator only, in order to test the intrinsic reactivity of these various

0024-9297/89/2222-4455$01.50/0